Pure Appl. Chem., Vol. 84, No. 12, pp. 2569–2578, 2012.
http://dx.doi.org/10.1351/PAC-CON-12-02-07

Efficient synthesis and self-assembly of hetero-grafted amphiphilic polypepide bottlebrushes*

Chunhui Luo, Chongyi Chen, and Zhibo Li‡

Beijing National Laboratory for Molecular Sciences (BNLMS), Institute of Chemistry, Chinese Academy of Sciences, Beijing 100190, China

Abstract: A new type of hetero-grafted molecular bottlebrush with polypeptide as backbone was synthesized using graft-onto strategy. Poly(γ-propargyl-L-glutamate) (PPLG) as backbone was firstly synthesized via ring-opening polymerization (ROP) of γ-propargyl-L-glutamate (PLG) N-carboxyanhydride (NCA). Next, polystyrene-N_3 (PS-N_3) and monomethoxy poly(ethylene glycol)-N_3 (mPEG-N_3) as side chains were grafted onto the PPLG backbone using copper-catalyzed click reaction, which afforded good grafting density and efficiency. Two polypeptide bottlebrushes with PS-to-mPEG molar ratio at 70/30 and 30/70 were prepared. The self-assembly behaviors of these two polypeptide bottlebrushes were investigated using the cosolvent method, and their supramolecular structures were characterized using light scattering (LS) and electron microscopy.

Keywords: amino acids; bottlebrushes; click chemistry; macromolecular chemistry; polypeptides; polymer chemistry; ring-opening reactions; self-assembly.

INTRODUCTION

Molecular bottlebrushes as a unique macromolecular architecture receive extensive research interest [1–3]. Generally, three synthetic strategies, i.e., graft-through, graft-onto, and graft-from, were applied to make bottlebrushes. In addition to simple bottlebrush containing single component, different polymer chemistry methods were combined to make more complicated architectures such as block copolymer bottlebrushes, core-shell bottlebrushes, hybrid materials, and toothbrush-like bottlebrushes [4–17]. However, most cases involved nondegradable backbones. Recently, great research efforts have contributed to polypeptide-based molecular bottlebrushes considering their unique secondary structures and good biodegradability [18–21]. Compared to flexible polymer coil, polypeptides can adopt rigid helical conformation to allow high grafting density [6], which was hardly obtainable using classical graft-onto method due to steric hindrance [7]. For example, Hammond's group reported quantitative grafting of poly(ethylene glycol) (PEG) onto poly(γ-propargyl-L-glutamate) (PPLG) backbone [6]. Recently, Zhang and co-workers described a rather general route to prepare side-chain-functionalized polypeptide based on γ-chloropropyl-L-glutamate [10,15]. Chen et al. and our group reported synthesis of molecular bottlebrushes with polypeptide backbone via ring-opening polymerization (ROP) and atom-transfer radical polymerization (ATRP) [12–14].

Pure Appl. Chem.* **84, 2499–2675 (2012). A collection of invited papers based on presentations at the 7th International Conference on Novel Materials and their Synthesis (NMS-VII) and the 21st International Symposium on Fine Chemistry and Functional Polymers (FCFP-XXI), Shanghai, China, 16–21 October 2011.
‡Corresponding author: E-mail: zbli@iccas.ac.cn

It is well known that amphiphilic block copolymers can self-assemble into ordered nano-objects such as micelles and vesicles, which might have great potential in biomedical applications. On the other hand, increasing interest has been paid to the self-assembly behaviors of hetero-grafted molecular bottlebrushes, which can exhibit high complexity compared to linear block copolymers, in a closer step to mimic biological system. For example, Wooley and co-workers reported the synthesis of hetero-grafted diblock molecular bottlebrushes that can form micelles in selective solvent [9]. Later, they developed a hierarchical process and realized dynamic cylindrical nanostructures [16]. Rzayev's group obtained well-defined nanotubes from multicomponent bottlebrush copolymers by a combination of different living polymerization methods [17]. Lin's group found PBLG-graft-PEG (PBLG-g-PEG) copolymer can self-assemble into spherical micelles, spindle-like micelles, and vesicles under appropriate conditions [4,5,22,23]. Although several amphiphilic bottlebrushes were reported, self-assembly behaviors of hetero-grafted molecular brushes with rigid polypeptide-backbone were still rare.

Herein, we report a highly efficient, one-pot graft-onto process to prepare hetero-grafted amphiphilic polypeptide bottlebrush. PPLG is firstly prepared via controlled ROP of functional N-carboxyanhydride (NCA). Azide end-functionalized polystyrene (PS-N_3) and monomethoxy poly(ethylene glycol) (mPEG-N_3) at different molar ratio are clicked onto PPLG backbone to give target polypeptide bottlebrush. The synthesis routes are illustrated in Scheme 1. Furthermore, the self-assembly behaviors of obtained amphiphilic polypeptide bottlebrush are investigated. We find that these molecular brushes can form micelles, cylinders, or vesicles depending on sample composition and cosolvent compositions.

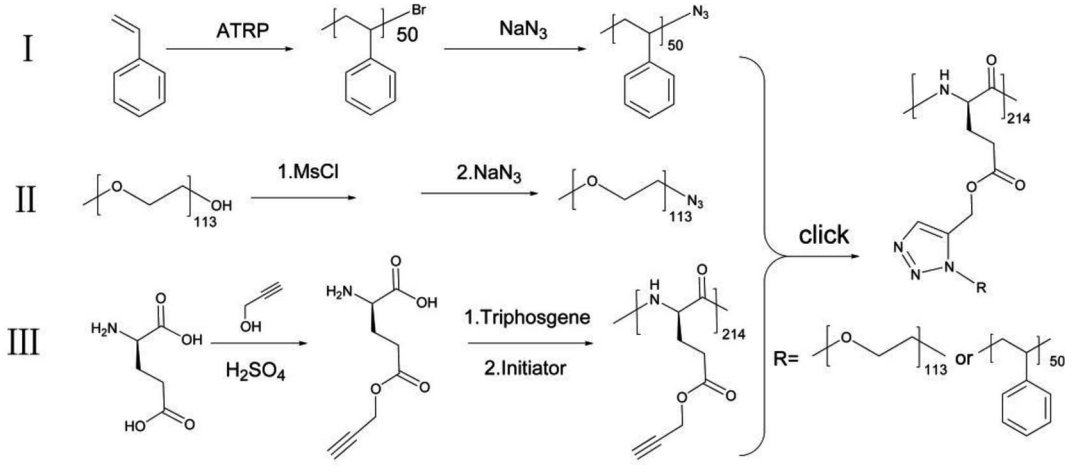

Scheme 1 Synthetic routes to hetero-grafted PPLG-g-(PS_{50}+$mPEG_{113}$) bottlebrushes.

EXPERIMENTAL SECTION

Materials

$mPEG_{113}$ (M_n = 5000 Da), propargyl alcohol (98 %) were purchased from Aldrich. L-Glutamic acid was obtained from GL Biochem (Shanghai) Ltd. All organic solvents were purchased from Beijing Chemical Co. Dichloromethane (DCM), tetrahydrofuran (THF), and *n*-hexane were purified by first purging with dry nitrogen, followed by passing through columns of activated alumina. *N*,*N'*-dimethylformamide (DMF) was treated with free amine scavenger (Aldrich) before being passed through 4 Å molecular sieves and activated alumina column. Deionized (DI) water (18 MΩ-cm) was obtaining from

a Millipore Milli-Q purification unit. Styrene (98 %, Aldrich) was stirred over CaH_2 overnight and distilled under reduced pressure.

Synthesis of γ-propargyl-L-glutamate (PLG)

PLG was prepared by direct coupling between propargyl alcohol and L-glutamic acid via sulfuric-acid-catalyzed esterification (Scheme 1) [6,12]. To a solution of L-glutamic acid (20 g) suspended in propargyl alcohol (30 mL) at 0 °C, 8 mL sulfuric acid was added drop-wise over 20 min. The solution was stirred at room temperature overnight before neutralized with excess 5 wt % $NaHCO_3$ aqueous solution. White solid appeared and was collected by centrifugation. The product was then dispersed in methanol, and the mixture was filtered again to remove insoluble compound. The filtrate was combined, and the solvent was removed using rotary-evaporator to give white solid in 38 % yield. ^{1}H NMR (400 MHz, D_2O): δ = 2.17–2.29 (m, 2H, $CHCH_2CH_2$), 2.55–2.66 (m, 2H, $CHCH_2CH_2$), 2.93 (t, 1H, C≡C*H*), 3.81 (t, 1H, $CHCH_2CH_2$), 4.76 (d, 2H, $OCH_2C{\equiv}CH$).

Synthesis of PLG-NCA

After purification, the PLG monomer was then converted into corresponding α-amino acid NCA using triphosgene in THF [6]. The obtained NCA was viscous oil at room temperature and difficult to purify using traditional recrystallization strategy. Flash column chromatography [24] was used to purify PLG-NCA after three precipitations in THF/hexane mixture. The isolated yield is 20 %. ^{1}H NMR (400 MHz, $CDCl_3$): δ = 2.17–2.29 (m, 2H, $CHCH_2CH_2$), 2.51 (t, 1H, C≡C*H*), 2.60–2.71 (m, 2H, $CHCH_2CH_2$), 4.41 (t, 1H, $CHCH_2CH_2$), 4.72 (d, 2H, $OCH_2C{\equiv}CH$), 6.27 (s, br, 1H, N*H*).

Synthesis of PPLG-g-(PS_{50}+$mPEG_{113}$)

PS_{50}-N_3 [M_n(GPC) = 5000 Da, polydispersity index (PDI) = 1.05] and $mPEG_{113}$-N_3 were synthesized and purified following the reported procedure [7,8]. PPLG was obtained by ROP of PLG-NCA using the Ni(COD)depe complex as initiator [25]. The yield is 85 % with degree of polymerization (DP) being 214. [M_n(GPC/LLS) = 36 000 Da, PDI = 1.11]. ^{1}H NMR (400 MHz, $CDCl_3$): δ = 2.02–2.86 (br, $CHCH_2CH_2$, C≡C*H*, and CH_2CH_2COO), 3.94 (br, 1H, $CHCH_2CH_2$), 4.68 (br, 2H, $OCH_2C{\equiv}CH$), 8.30 (br, 1H, N*H*).

PPLG was then coupled with $mPEG_{113}$-N_3 and PS_{50}-N_3 using $CuSO_4{\cdot}5H_2O$/sodium ascorbate as catalyst in DMF with a molar ratio of alkyne/azide/sodium ascorbate/$CuSO_4{\cdot}5H_2O$ = 1.1:1:1:0.2. The feeding ratio of PS/mPEG was fixed at 3:7 and 7:3 (molar ratio) to give two polypeptide bottlebrushes designated as **H1** and **H2**, respectively. After 5 h, the reaction solution was passed through an aluminum oxide column to remove the catalyst. After that, DMF was removed under reduced pressure before DCM was added to dissolve the polymer. The target products were purified by precipitation in excess petroleum ether and characterized using ^{1}H NMR spectroscopy, gel permeation chromatography (GPC), and circular dichroism (CD). The results are summarized in Table 1.

Table 1 Molecular parameters of homopolymers and polypeptide bottlebrushes.

Sample	M_n (kDa)[a]	PDI	M_n (kDa)[b]	PS:mPEG molar ratio	
				Theory	Experimental
$PPLG_{214}$	36.0	1.11	–	–	–
PS_{50}-N_3	5.0	1.05	4.9	–	–
H1	700.4	1.27	1006.6	3:7	3.1:6.9
H2	716.1	1.35	1008.7	7:3	7.0:3.0

[a]Determined from GPC/LLS.
[b]Determined from NMR.

Sample preparation

H1 and **H2** bottlebrush samples were firstly dissolved in DMF to make a stock solution with concentration of 0.5 wt %. Predetermined amount of DI water (e.g., 9 or 41 wt %) was then added slowly to the stock solution under stirring to induce self-assembly of **H1** or **H2** bottlebrushes. We defined initial water content at 9 wt % as condition I and 42 wt % as condition II. The solution was aged at room temperature for 24 h before adding excess water to quench the supramolecular structures. The final concentration was 0.1 wt %. After that, DMF was then removed by exhaustive dialysis against DI water for 72 h with water change every 12 h.

Characterization

^{1}H NMR spectra were recorded on Bruker AV400 FT-NMR spectrometer (at 400 MHz). Tandem GPC/laser light scattering (GPC/LLS) was performed at 50 °C using an SSI pump connected to Wyatt Optilab DSP and Wyatt DAWN EOS LS detectors with DMF containing 0.02 M LiBr as eluent. The flow rate was 1.0 mL/min. All GPC/LLS samples were prepared at concentrations of about 5 mg/mL. Dynamic light scattering (DLS) and static light scattering (SLS) measurements were performed using LLS spectrometer (ALV/DLS/SLS-5322F) equipped with a multi-τ digital time correlator (ALV5000) and a He-Ne Laser (λ = 632.8 nm) from 30 to 150º. Apparent diffusion coefficients (D_{app}) were obtained from the slope of the decay rate (Γ) vs. the square of scattering vector (q) using $\Gamma = D_{app}q^2$. Hydrodynamic radius (R_h) was then calculated using the Stokes–Einstein equation. A Zimm plot was used to calculate the radius of gyration (R_g). Transmission electron microscopy (TEM) samples were prepared by casting dilute sample solution on carbon-coated TEM grids and left to dry over night, then characterized on a JEOL JEM-2200FS TEM operating at 200 kV. CD spectra were recorded on an Applied Photophysics Chirascan CD Spectrometer. The solution was placed into a quartz cell with a path length of 0.1 cm.

RESULTS AND DISCUSSION

Synthesis of PPLG-g-(PS_{50}+$mPEG_{113}$) bottlebrushes

Three reactive polymer precursors, i.e., $PPLG_{214}$, PS_{50}-N_3, and $mPEG_{113}$-N_3, were prepared and purified following literature procedures (Scheme 1) [6–8]. Their molecular weight and molecular weight distributions were determined using GPC/LLS, and their structures were verified using ^{1}H NMR and Fourier transform infrared (FTIR) spectroscopy. The characteristic resonances are well resolved, and corresponding integral ratio agrees well with expected structures [6]. Note that the PLG-NCA was purified using flash column chromatography [24] after three times precipitation in THF/hexane. The obtained PLG-NCA has adequate purity to allow controlled ROP polymerization. We attempted to poly-

merize using different initiator systems, including primary amine, tertiary amine, transition-metal complex, and hexamethyldisilazane, for ROP of PLG-NCA [25–27]. All can initiate PLG-NCA polymerization in mild conditions. We chose the Ni(COD)depe complex in DMF for this study. The obtained M_n from GPC/LLS is 36.0 kDa (DP = 214) with PDI = 1.11. Also, the obtained PPLG is confirmed by ^{1}H NMR spectroscopy shown in Fig, 1b, which is consistent with the literature report [6].

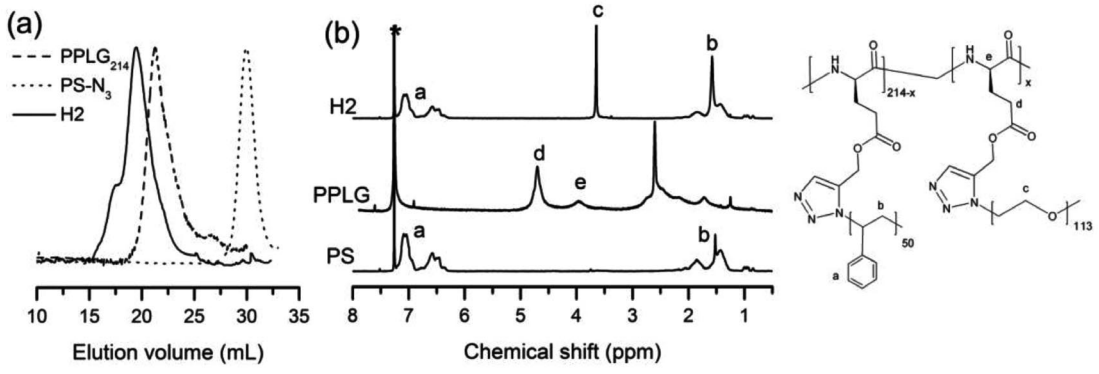

Fig. 1 (a) GPC traces of PS_{50}-N_3, $mPEG_{113}$-N_3, $PPLG_{214}$, and **H2** bottlebrush; (b) ^{1}H NMR spectra of PS_{50}-N_3, $PPLG_{214}$, and molecular brush **H2** in $CDCl_3$.

Next, PS_{50}-N_3 and $mPEG_{113}$-N_3 are clicked with $PPLG_{214}$ in the presence of copper catalyst [28,29]. Note that the PS and mPEG chains are presumably randomly conjugated to the PPLG backbone via copper-catalyzed click reaction. However, we do not have a good method to characterize this. Figure 1a shows GPC traces of $PPLG_{214}$, PS-N_3, and hetero-grafted bottlebrushes (**H2**), respectively. Compared with $PPLG_{214}$, **H2** displays apparent decrease of elution volume, indicating a successful grafting of PS and mPEG chains on PPLG backbone. In this reaction, PS_{50}-N_3 and $mPEG_{113}$-N_3 are limiting agents with alkyne/azide molar ratio being 1.1. Using this method, we prepared two hetero-grafted PPLG-g-(PS_{50}+$mPEG_{113}$) bottlebrushes with PS-to-mPEG ratio at 70:30 and 30:70, respectively, which are designated as **H1** and **H2** for the following text. ^{1}H NMR characterizations demonstrate that the polymer compositions are almost the same with feed ratio, indicating a high grafting efficiency. The corresponding molecular weights are summarized in Table 1.

Since these bottlebrushes have polypeptide as backbone, it is interesting to determine the secondary structures of **H1** and **H2** in nonselective solvent. The secondary structure of PPLG, **H1**, and **H2** in THF are characterized using CD spectroscopy (Fig. 2). PPLG shows two characteristic minimum at 208 and 222 nm, indicating an α-helical conformation [30]. The helicity is close to 100 % using PBLG as reference. Notably, introduction of PS and mPEG as side chains substantially decreases the helical regularity as revealed from CD analysis shown in Fig. 2. If taking PPLG as reference, the helicity of **H1** and **H2** decreased to 30 % and 36 %, respectively. We believe that the reason is that steric repulsion of side chains could destabilize the helical structures [6,14,15]. Such effects were also observed in poly(γ-chloropropyl-L-glutamate) system reported by Zhang et al.

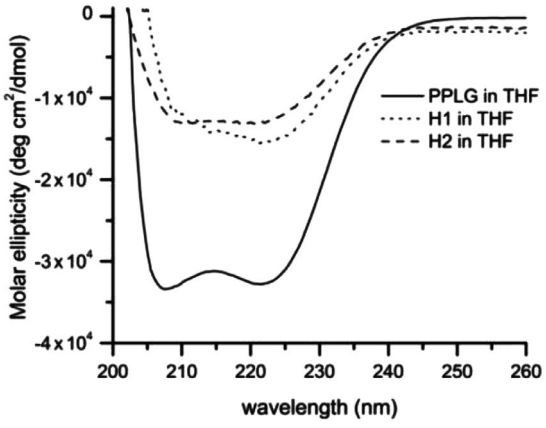

Fig. 2 CD spectra of PPLG, hetero-grafted molecular brush **H1** and **H2** in THF at room temperature.

Self-assembly of PPLG-g-(PS_{50}+$mPEG_{113}$) in water

The self-assembly of amphiphilic **H1** and **H2** bottlebrushes are investigated using the cosolvent method [31–34]. Previous studies showed that the water content between 5.5 and 9.5 wt % was a suitable range to investigate the self-assembly of copolymers containing PS segments [33]. Here, we thus explore the self-assembly of hetero-grafted polypeptide bottlebrushes in DMF/H_2O mixture containing 9 wt % water.

We firstly applied DLS to determine the apparent aggregate size and distributions under condition I. We tried using multi-angle DLS to determine the decay rate (Γ) dependence on scattering angles, and found that the decay rate (Γ) did not show strong dependence on the scattering angle. Also considering the obtained assemblies are polydisperse, we thus simply use the R_h at 90º for remaining discussion. For **H1**, hydrophilic PEG is the major components, i.e., 70 wt %. DLS measurement gives R_h of 40 nm with PDI = 0.178 at an angle of 90º (Fig. 3a). TEM examination on the same solution reveals that spherical aggregates are the main structures (Fig. 4a), although the micelle size (radius) from TEM is about 7 nm, which is much smaller than DLS results. We presume the smaller size is due to dehydration of PEG side chain when casting sample solution on carbon film. We further performed SLS to determine R_g for the same sample. From these data, we can roughly estimate R_g being 32 nm for **H1** bottlebrushes using a Zimm treatment. Combining results from DLS and SLS, we estimate the $\langle R_g \rangle / \langle R_h \rangle$ ratio for **H1** being 0.80, close to 0.77 for hard-sphere aggregate [35–37], further confirmed the spherical micelles for **H1** formed under condition I.

In contrast, **H2** bottlebrush contains 70 % hydrophobic PS_{50} as side chains. Its solubility in water is expected to be lower than sample **H1**. We firstly explored its self-assembly behaviors under condition I. The R_h from DLS at an angle of 90º is about 76 nm with PDI = 0.26 (Fig. 3b), while TEM examination gives aggregates size (radius) being 13 nm (Fig. 4b). Given the contour length of PS_{50} around 12 nm, this indicates the PS blocks were highly stretched in the **H2** sample. In addition, R_g from SLS measurements for **H2** bottlebrush is about 55 nm, which gives $\langle R_g \rangle / \langle R_h \rangle$ ratio being 0.72, further confirmed spherical morphology [35–37].

It is well known that the assembly morphology of amphiphilic copolymers is not only determined by copolymer composition, but also solvent polarity [31–34]. For a same copolymer, increase in solvent polarity can induce micelle morphology transition from sphere to cylinder and to vesicle [32]. We initially tried using DMF/H_2O cosolvent with low water content, i.e., 9 wt %. Since water is a poor solvent for the PS segment, increase of initial water content in DMF/H_2O mixture will certainly increase solvent selectivity for self-assembly of **H1** and **H2** bottlebrushes. Therefore, we increased the

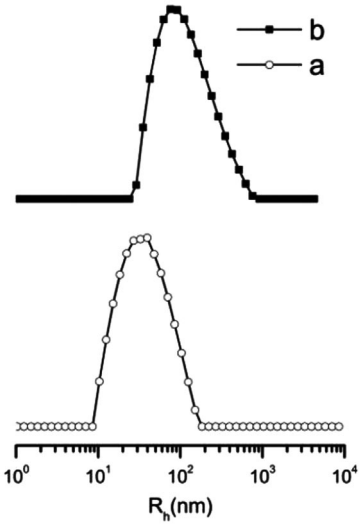

Fig. 3 Apparent size distributions of (a) **H1** and (b) **H2** hetero-grafted bottlebrushes in dilute aqueous solutions (0.1 wt %) prepared under condition I. The scattering angle is 90º.

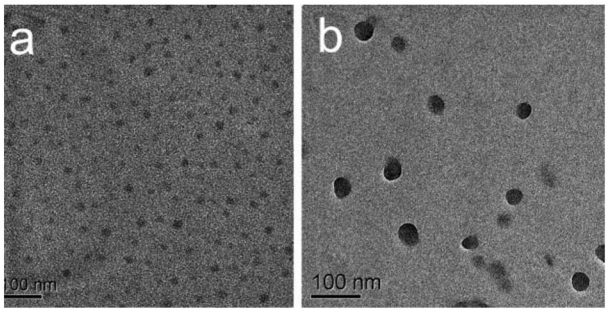

Fig. 4 TEM images of (a) **H1** and (b) **H2** hetero-grafted bottlebrushes in dilute aqueous solutions (0.1 wt %) prepared under condition I.

initial water percentage to 41 wt % before adding excess water to quench the resulting supramolecular morphology.

DLS is then applied to characterize the aggregate size and size distributions (Fig. 5) under condition II. For **H1** bottlebrush containing more hydrophilic PEG side chains than hydrophobic PS side chains, DLS measurements reveal that R_h is 89 nm with PDI = 0.345, which is much larger than those formed in cosolvent under condition I. DLS also suggests the aggregates have broad distribution. SLS measurement of the same solution gives R_g being 133 nm. Taking DLS and SLS data together, we obtain $\langle R_g \rangle / \langle R_h \rangle$ ratio of 1.49, which is indicative of cylindrical morphology [35–37]. TEM characterization in Fig. 6a verifies that the short cylinder becomes the predominate morphology for the **H1** solution. Typically, the cylinder sizes range between 60 and 130 nm.

For **H2** bottlebrush, R_h from DLS at an angle of 90º is 78 nm under condition II. Notably, increase of initial water content for **H2** bottlebrush does not cause obvious change of aggregate sizes from DLS measurements. TEM characterization on this solution indicates vesicular morphology for **H2** bottlebrush assembled under condition II (Fig. 6b). The vesicle size (radius) ranges from 50 to 65 nm, and the vesicle membrane thickness is about 25 nm, indicating bilayer arrangements of highly stretched

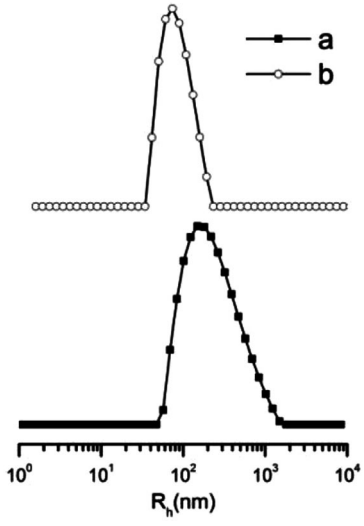

Fig. 5 Apparent size distributions of (a) **H1** and (b) **H2** hetero-grafted bottlebrushes in dilute aqueous solutions (0.1 wt %) prepared under condition II. The scattering angle is 90º.

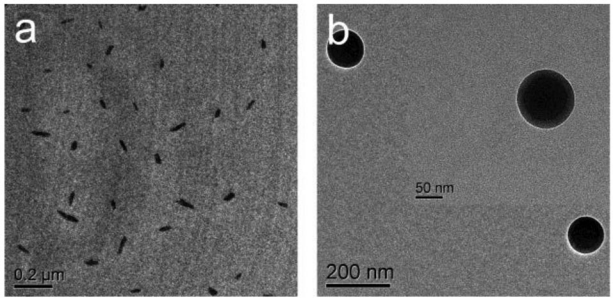

Fig. 6 TEM images of (a) **H1** and (b) **H2** hetero-grafted molecular brushes aqueous solutions (0.1 wt %) prepared under condition II.

PS blocks. Further, SLS measurements reveal R_g of these aggregates being 72 nm. Taking the DLS and SLS data together, we then obtain $<R_g>/<R_h> = 0.92$, close to the theoretical value for vesicle (1.0) [35–37]. In addition to TEM results, multi-angle DLS and SLS characterization also verify the vesicular structures.

We have demonstrated that **H1** and **H2** bottlebrushes with polypeptide as backbone can self-assemble into spherical, cylindrical, and vesicular structures depending on cosolvent composition. For amphiphilic block copolymer, the assembly morphology dependence on copolymer composition and solvent properties as well as method of assembly method has been well explored both experimentally and theoretically [32,33,38–42]. Previous studies already showed that a simple poly(styrene-*b*-dimethylsiloxane) diblock could form sphere, cylinder, and vesicle in different polar solvents due to different degree of swelling for solvophobic block [40]. Furthermore, the incomplete graft of side chains provides semi-flexibility onto the peptide backbone, which can bend for the hydrophobic PS blocks to form the core of micelles in water [4]. Taking this information together, we propose a mechanism of such transition shown in Scheme 2. At 9 wt % water content, the solvent was partially selective for PS blocks. As a result, only spherical micelles were observed regardless of polymer composition. In contrast, as water content increased to 41 wt %, the spherical micelles transited to new morphology to min-

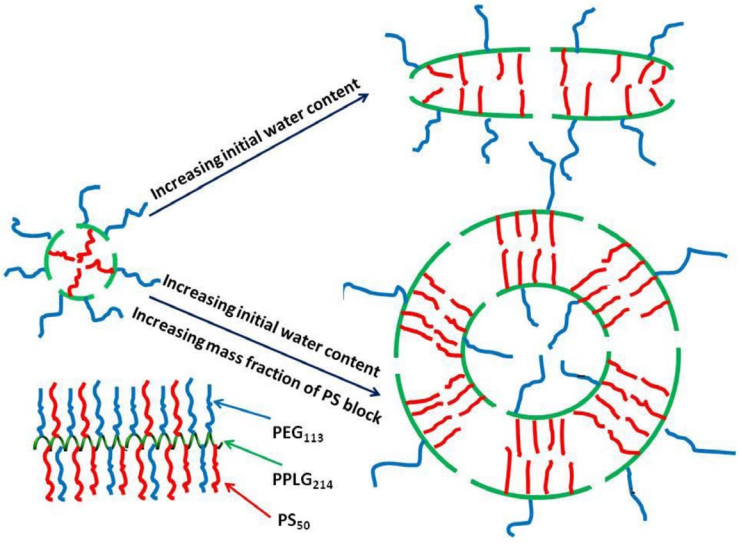

Scheme 2 Schematic illustration of the re-assembly of hetero-grafted molecular brushes in water.

imize free energy. In this case, **H1** containing 30 % hydrophobic PS prefers forming cylindrical micelles, while **H2** containing 70 % hydrophobic PS intends to form vesicles. Our results were consistent with the literature report. For example, Eisenberg and Shen observed that polystyrene-*b*-polyacrylic acid diblock copolymer formed spheres in dioxane/H_2O containing 10 % water, but the micelle morphology transformed into vesicles when water content increased to 40 % [41]. Bates and co-workers demonstrated that poly(1,2-butadiene-*b*-poly(ethylene oxide) (PB-PEO) diblock copolymer mainly formed cylindrical micelles when the mass fraction of hydrophobic PB block was between 30~65 %. But the micelle morphology changed to vesicles when the mass fraction of PB was higher than 65 % [42].

CONCLUSION

In summary, we demonstrated a facile method of preparing hetero-grafted bottlebrushes with polypeptide as backbone via ROP and click reaction. The synthesis of the brushes as well as their self-assembly behaviors in aqueous solution were studied. The grafting of side chains did affect the secondary structure of polypeptide backbone. Also, we found that these hetero-grafted bottlebrushes can form spherical micelles, cylinders, and vesicles depending on sample and cosolvent compositions. The supramolecular assemblies have degradable polypeptide domains.

ACKNOWLEDGMENTS

The authors appreciate financial support from the National Natural Science Foundation of China (50821062, 91027043), the Chinese Academy of Sciences (KJCX2-YW-H19).

REFERENCES

1. S. S. Sheiko, B. S. Sumerlin, K. Matyjaszewski. *Prog. Polym. Sci.* **33**, 759 (2008).
2. M. F. Zhang, A. H. E. Müller. *J. Polym. Sci. Part A: Polym. Chem.* **43**, 3461 (2005).
3. H.-i. Lee, J. Pietrasik, S. S. Sheiko, K. Matyjaszewski. *Prog. Polym. Sci.* **35**, 24 (2010).
4. C. Cai, J. Lin, T. Chen, X. Tian. *Langmuir* **26**, 2791 (2009).

5. W. Ding, S. Lin, J. Lin, L. Zhang. *J. Phys. Chem. B* **112**, 776 (2007).
6. A. C. Engler, H.-i. Lee, P. T. Hammond. *Angew. Chem., Int. Ed.* **48**, 9334 (2009).
7. H. Gao, K. Matyjaszewski. *J. Am. Chem. Soc.* **129**, 6633 (2007).
8. B. Parrish, R. B. Breitenkamp, T. Emrick. *J. Am. Chem. Soc.* **127**, 7404 (2005).
9. Z. Li, J. Ma, C. Cheng, K. Zhang, K. L. Wooley. *Macromolecules* **43**, 1182 (2010).
10. H. Tang, D. Zhang. *Biomacromolecules* **11**, 1585 (2010).
11. C. Chen, Z. Wang, Z. Li. *Biomacromolecules* **12**, 2859 (2011).
12. J. Ding, C. Xiao, Z. Tang, X. Zhuang, X. Chen. *Macromol. Biosci.* **11**, 192 (2011).
13. J. Ding, C. Xiao, L. Zhao, Y. Cheng, L. Ma, Z. Tang, X. Zhuang, X. Chen. *J. Polym. Sci., Part A: Polym. Chem.* **49**, 2665 (2011).
14. Y. Liu, P. Chen, Z. Li. *Macromol. Rapid Commun*. **33**, 287 (2012).
15. H. Tang, Y. Li, S. H. Lahasky, S. S. Sheiko, D. Zhang. *Macromolecules* **44**, 1491 (2011).
16. Z. Li, J. Ma, N. S. Lee, K. L. Wooley. *J. Am. Chem. Soc.* **133**, 1228 (2011).
17. K. Huang, J. Rzayev. *J. Am. Chem. Soc.* **131**, 6880 (2009).
18. M. A. Gauthier, H. A. Klok. *Chem. Commun*. 2591 (2008).
19. L. A. Canalle, D. Lowik, J. C. M. van Hest. *Chem. Sov. Rev.* **39**, 329 (2010).
20. D. Timothy. *J. Prog. Polym. Sci.* **32**, 858 (2007).
21. N. Hadjichristidis, H. Iatrou, M. Pitsikalis, G. Sakellariou. *Chem. Rev*. **109**, 5528 (2009).
22. D. Tang, J. Lin, S. Lin, S. Zhang, T. Chen, X. Tian. *Macromol. Rapid Commun.* **25**, 1241 (2004).
23. C. Cai, J. Lin, T. Chen, X.-S. Wang, S. Lin. *Chem. Commun.* 2709 (2009).
24. J. R. Kramer, T. J. Deming. *Biomacromolecules* **11**, 3668 (2010).
25. T. J. Deming. *Nature* **390**, 386 (1997).
26. H. R. Kricheldorf. *Angew. Chem., Int. Ed.* **45**, 5752 (2006).
27. H. Lu, J. Cheng. *J. Am. Chem. Soc*. **129**, 14114 (2007).
28. H. C. Kolb, M. G. Finn, K. B. Sharpless. *Angew. Chem., Int. Ed*. **40**, 2004 (2001).
29. Y. L. Angell, K. Burgess. *Chem. Soc. Rev*. **36**, 1674 (2007).
30. P. Y. Chou, G. D. Fasman. In *Advances in Enzymology and Related Areas of Molecular Biology*, pp. 45–148, John Wiley, New York (2006).
31. B. Guan, M. Jiang, X. G. Yang, Q. Liang, Y. Y. Chen. *Soft Matter* **4**, 1393 (2008).
32. A. Choucair, A. Eisenberg. *Eur. Phys. J. E* **10**, 37 (2003).
33. L. Zhang, A. Eisenberg. *Macromolecules* **32**, 2239 (1999).
34. L. Zhang, A. Eisenberg. *Science* **268**, 1728 (1995).
35. S. U. Egelhaaf, P. Schurtenberger. *J. Phys. Chem*. **98**, 8560 (1994).
36. W. Burchard. *Adv. Polym. Sci*. **48**, 1 (1983).
37. N. C. Santos, M. A. Castanho. *Biophys. J.* **71**, 1641 (1996).
38. Y.-Y. Won, A. K. Brannan, H. T. Davis, F. S. Bates. *J. Phys. Chem. B* **106**, 3354 (2002).
39. G. Srinivas, D. E. Discher, M. L. Klein. *Nat. Mater*. **3**, 638 (2004).
40. J. Bang, S. Jain, Z. Li, T. P. Lodge, J. S. Pedersen, E. Kesselman, Y. Talmon. *Macromolecules* **39**, 1199 (2006).
41. H. Shen, A. Eisenberg. *Macromolecules* **33**, 2561 (2000).
42. S. Jain, F. S. Bates. *Science* **300**, 460 (2003).